

비압축성 물체의 수치해 안정화 기법
A Pressure Stabilization Technique for Incompressible Materials

이 상호*
Lee, Sang-Ho

김 상호**
Kim, Sang-Hyo

ABSTRACT

Mixed finite element formulations for incompressible materials show *pressure oscillations* or *pressure modes* in four-node quadrilateral elements. The criterion for the stability in the pressure solution is the so-called Babuška-Brezzi stability condition, and the four-node elements based on mixed variational principles do not appear to satisfy this condition. In this study, a pressure continuity residual based on the pressure discontinuity at element edges is used to study the stabilization of pressure solutions in bilinear displacement-constant pressure four-node quadrilateral elements. It is shown that the pressure solutions, although stable, exhibit sensitivity to the stabilization parameters.

1. Introduction

The four-node quadrilateral element is the workhorse of nonlinear finite element analysis because of its simplicity and versatility. However, when the element is implemented with full quadrature, it locks for incompressible materials in a phenomenon called *volumetric locking*. One remedy for this difficulty is selective-reduced integration, Hughes (1977). When this procedure is applied to volumetric locking, the hydrostatic, or pressure terms are integrated using a single quadrature point, whereas the deviatoric terms are evaluated by full quadrature. It became clear subsequently through the discovery of the equivalence principle by Malkus and Hughes (1978).

In the past decade, the performance of the quadrilateral element has been enhanced by using two field (Hellinger-Reissner) and three field (Hu-Washizu) variational principles. MacNeal (1993) shows an extensive account of the mechanics of overcoming volumetric locking. When the displacement of the nodes is such that the volume of the element is preserved, the strain field is equivolumental throughout the element. This is the key to avoiding volumetric locking. Unfortunately, a byproduct of designing this property into the strain field is that the element then fails to meet the Babuška-Brezzi conditions. As a consequence, in some meshes, the pressures alternate in sign in a phenomenon called *checkerboarding*, wherein

* 연세대학교 토목공학과 조교수

** 연세대학교 토목공학과 부교수

the pressures alternate. This malady is a result of the rank-deficiency of the equations for the pressure.

Hughes and Franca (1987) have developed a new methodology whereby the pressure oscillations are eliminated by adding the squares of the equilibrium equations and pressure discontinuities to the variational principle. However, in the use of this formulation, the relationship between the accuracy of displacement and pressure solutions and the stability parameter needs detailed study. In this paper, the Hughes-Franca stabilization procedure and the sensitivity of solutions will be studied in the four-node quadrilateral elements.

2. Incompressible Elasticity Formulation for the Stabilization of Pressure

The standard displacement-pressure formulation of isotropic incompressible elasticity is:

$$\operatorname{div} \boldsymbol{\sigma} + \mathbf{b} = 0 \quad \text{in } \Omega, \quad (1)$$

$$\operatorname{div} \mathbf{u} = 0 \quad \text{in } \Omega, \quad (2)$$

$$\boldsymbol{\sigma} = 2\mu\boldsymbol{\epsilon} - p\mathbf{I} \quad \text{in } \Omega, \quad (3)$$

$$\mathbf{u} = \mathbf{u}^* \quad \text{on } \Gamma_u, \quad \boldsymbol{\sigma} \cdot \mathbf{n} = \mathbf{t}^* \quad \text{on } \Gamma_t. \quad (4)$$

Here $\boldsymbol{\sigma}$ is the Cauchy stress tensor, \mathbf{b} is body force, \mathbf{u} is displacement (or velocity in fluid mechanics), μ is shear modulus (or viscosity in fluid mechanics), p is pressure, \mathbf{I} is the identity tensor, and $\boldsymbol{\epsilon}$ is the symmetric part of the displacement gradient. Equation (2) gives the incompressibility condition.

The weak form for isotropic incompressible materials is

$$\int_{\Omega} \delta\boldsymbol{\epsilon}^T 2\mu\boldsymbol{\epsilon} \, d\Omega - \int_{\Omega} \delta(\operatorname{div} \mathbf{u})^T p \, d\Omega - \int_{\Omega} \delta p (\operatorname{div} \mathbf{u}) \, d\Omega = \int_{\Omega} \delta\mathbf{u}^T \mathbf{b} \, d\Omega + \int_{\Gamma_t} \delta\mathbf{u}^T \mathbf{t}^* \, d\Gamma \quad (5)$$

This weak formulation is not stable for pressure solutions unless specific displacement and pressure interpolations are chosen. In particular, *pressure oscillations*, or *pressure modes* (often called checkerboarding) occur in the bilinear displacement-constant pressure four-node quadrilateral element (Q1P0).

Hughes and Franca (1987) modified the weak formulation as follows to stabilize the pressure

$$\begin{aligned} & \int_{\Omega} \delta\boldsymbol{\epsilon}^T 2\mu\boldsymbol{\epsilon} \, d\Omega - \int_{\Omega} \delta(\operatorname{div} \mathbf{u})^T p \, d\Omega - \int_{\Omega} \delta p (\operatorname{div} \mathbf{u}) \, d\Omega \\ & - \int_{\tilde{\Omega}} \frac{\alpha h^2}{2\mu} \delta(\operatorname{div} \boldsymbol{\sigma})^T (\operatorname{div} \boldsymbol{\sigma}) \, d\Omega - \int_{\tilde{\Gamma}} \frac{\beta h}{2\mu} [[\delta p]][[p]] \, d\Gamma \\ & = \int_{\tilde{\Omega}} \left(\delta\mathbf{u}^T + \frac{\alpha h^2}{2\mu} \delta(\operatorname{div} \boldsymbol{\sigma})^T \right) \mathbf{b} \, d\Omega + \int_{\Gamma_t} \delta\mathbf{u}^T \mathbf{t}^* \, d\Gamma \end{aligned} \quad (6)$$

where α and β are nondimensional stabilization parameters ($\alpha \geq 0$ and $\beta \geq 0$), h is the length parameter of the mesh, and $[[\cdot]]$ is the jump operator. The domain $\tilde{\Omega}$ denotes element interiors, and $\tilde{\Gamma}$ consists of the element interfaces. The above weak formulation involves the addition of "least-squares" forms of the following residuals: the equilibrium equation residual and the pressure continuity residual on element interfaces. These terms render the formulation to be coercive, in contrast to the classic Galerkin formulation, and enable the Babuška-Brezzi condition (Babuška, 1971 and Brezzi, 1974) to be avoided. Thus this formulation can provide stable pressure solutions for seemingly arbitrary combinations of displacement and pressure interpolations. In the above formulation, however, a careful choice of the parameters is required to prevent a loss of accuracy in the solution.

3. QBI Element Formulation Using γ -Projection Operator

For isotropic incompressible materials, the stress $\boldsymbol{\sigma}$ can be split into two parts as

$$\sigma_{ij} = \tau_{ij} - p\delta_{ij}. \quad (7)$$

Here, τ_{ij} denotes the deviatoric stress given by $\tau_{ij} = 2\mu\varepsilon_{ij} \equiv 2\mu e_{ij}$ where e_{ij} is the deviatoric strain, p is the hydrostatic pressure defined as $p = -\frac{1}{\text{nsd}} \sigma_{ii}$, and δ_{ij} is the Kronecker delta.

The three-field Hu-Washizu variational principle for this material is

$$\Pi^{\text{HW}} = \int_{\Omega} \left[\frac{1}{2} \varepsilon_{ij} 2\mu \varepsilon_{ij} - \tau_{ij} (\varepsilon_{ij} - u_{(i,j)}) - pu_{i,i} \right] d\Omega - W^{\text{ext}}. \quad (8)$$

The matrix form of (8) with a pressure continuity residual for stabilization of pressure is

$$\Pi^{\text{HW}}(\mathbf{u}, \boldsymbol{\varepsilon}, \boldsymbol{\tau}, p) = \int_{\Omega} \left[\frac{1}{2} \boldsymbol{\varepsilon}^T \mathbf{D}^{\text{dev}} \boldsymbol{\varepsilon} - \boldsymbol{\tau}^T (\boldsymbol{\varepsilon} - \nabla_s \mathbf{u}) - p(\text{div } \mathbf{u}) \right] d\Omega - \frac{\bar{\beta}}{2} \int_{\tilde{\Gamma}} [[p]]^2 d\Gamma - W^{\text{ext}} \quad (9)$$

where $\bar{\beta} = \frac{\beta h}{2\mu}$. The above functional, when the pressure residual term is excluded, is the

standard Hu-Washizu form for incompressible materials where p is the Lagrange multiplier on the isochoric constraint $u_{i,i} = 0$. For nearly incompressible materials, a perturbed Lagrangian approach is taken where an additional term, $\frac{1}{2\lambda} p^2$, is added to the functional. Taking stationary condition then gives the following weak form (QBI-HF):

$$\int_{\Omega} \left[\delta \boldsymbol{\varepsilon}^T (\mathbf{D}^{\text{dev}} \boldsymbol{\varepsilon} - \boldsymbol{\tau}) - \delta \boldsymbol{\tau}^T (\boldsymbol{\varepsilon} - \nabla_s \mathbf{u}) - \delta p(\text{div } \mathbf{u}) + \delta (\nabla_s \mathbf{u})^T \boldsymbol{\tau} - \delta (\text{div } \mathbf{u})^T p \right] d\Omega - \bar{\beta} \int_{\tilde{\Gamma}} [[\delta p]][[p]] d\Gamma - \delta W^{\text{ext}} = 0. \quad (10)$$

4. Numerical Examples

The accuracy and the stability of displacement and pressure solutions in four-node quadrilateral elements will be studied for various values of the stability parameter β . Note that when the parameter β is equal to zero, i.e. $\bar{\beta} = 0$, the weak form (10) becomes the conventional formulations which fail the Babuška-Brezzi stability condition.

For the convergence study, the displacement norm (L_2 norm) can be calculated as

$$\text{displacement norm} = \left[\int_{\Omega} (\mathbf{u} - \mathbf{u}^h)^T (\mathbf{u} - \mathbf{u}^h) d\Omega \right]^{1/2}. \quad (11)$$

For incompressible plane strain, energy norm can be decomposed into the deviatoric energy norm and the pressure norm as

$$\text{deviatoric energy norm} = \left[\frac{1}{2} \int_{\Omega} (\boldsymbol{\varepsilon} - \boldsymbol{\varepsilon}^h)^T \mathbf{D}^{\text{dev}} (\boldsymbol{\varepsilon} - \boldsymbol{\varepsilon}^h) d\Omega \right]^{1/2}, \quad (12)$$

$$\text{pressure norm} = \left[\int_{\Omega} (\mathbf{p} - \mathbf{p}^h)^T (\mathbf{p} - \mathbf{p}^h) d\Omega \right]^{1/2}. \quad (13)$$

Timoshenko Beam Problem. The test problem is a linear, elastic cantilever with a load P at its end as shown in Fig. 1. In the convergence study of this beam problem, incompressible material or nearly incompressible materials are considered because both volumetric locking and pressure oscillations (or pressure modes) occur in this case. A state of plane strain is assumed.

The convergence rates of displacement norms by QBI-HF are shown in Fig. 2. The rates of convergence of displacement norms are approximately $O(h^2)$. The convergence rates of deviatoric energy norms and pressure norms are shown in Fig. 3 and 4, respectively. The rate of convergence is approximately $O(h^1)$.

The pressure solutions of QBI-HF for the prescribed displacement boundary conditions are shown in Fig. 5, where the pressure distributions at $x = 22.5$ for various values of β are compared with exact pressures. The pressure solutions of Simo-Rifai are also presented. The pressure solutions show an oscillation for $\beta \leq 0.0001$, and the solutions become erratic for $\beta > 0.1$. In other words, the pressure solutions are unstable for small β values, and they seem to be stable but not accurate for large β values in which the accuracy of displacement solutions is also poor. For the range of $0.001 \leq \beta \leq 0.1$, the pressure solutions are stable and accurate and the displacement solutions are accurate. These phenomena can be observed more clearly in the next example.

Pressure Modes in Timoshenko Beam Problem. In order to capture the pressure modes in the beam, the boundary condition at $x = 0$ is modified so that $u_y = 0$ at points B and C of Fig. 1. The introduction of this perturbation makes the pressure solutions of the beam problem highly oscillatory for unstable elements.

The pressure distributions at $x = 22.5$ for various values of β under the additional displacement perturbation condition are shown in Fig. 6. The pressure distributions of Simo-Rifai and other elements exhibit the *pressure modes* under this constraint condition. In Fig. 6, the pressure distributions for small β values ($\beta \leq 0.0001$) are not shown because the pressures oscillate severely. As β increases, the oscillations diminish and the pressure solutions become stable and accurate. For large β values ($\beta > 0.1$) the pressure solutions become erratic.

Driven Cavity Flow Problem. The last example is the well known driven cavity flow problem. The geometry of the model is shown in Fig. 7. Two different boundary conditions have been used; one of which, Case A (often called 'leaky lid' boundary condition), causes *pressure oscillations* and the other, Case B (often called 'ramp over one element' boundary condition), causes *pressure modes* in conventional finite element analyses. In this example, the stability parameter $\beta = 0.01$ was used.

The distribution of pressures at $y=0.35$ for QBI-HF and other several elements is shown in Fig. 8 where the boundary condition Case A has been used. The smoothed curve obtained by post processing, see (Lee et al., 1979), is considered as the benchmark solution. The pressures of QM6, Simo and Rifai's element and ASQBI are oscillatory whereas those of QBI-HF are stable and accurate. The distribution of pressures in the boundary condition Case B is shown in Fig. 9. This boundary condition makes the pressure solutions of conventional methods more unstable. The pressures of QM6, Simo and Rifai's element, and ASQBI show severe *checkerboarding* and could not be shown in Fig. 9 without obscuring the benchmark solution. The pressures of QBI-HF are also stable in this case.

5. Conclusions

The stabilization procedure of Hughes and Franca has been studied in the context of a four-node quadrilateral element with a strain field designed to avoid volumetric locking. It has been shown that this stabilization avoids the pressure oscillations which plague these elements for incompressible materials. The sensitive of the stabilization parameter is summarized below:

1) For $0 < \beta \leq 0.001$: *Pressure oscillations* or *pressure modes* can not be eliminated successfully.

2) For $0.001 < \beta \leq 0.1$: *Pressure oscillations* or *pressure modes* are eliminated successfully. Pressure solutions are stable and accurate. Displacement solutions are still accurate (there is no significant loss of accuracy in the displacement solutions).

3) For $0.5 \leq \beta \leq 10.0$: *Pressure oscillations* or *pressure modes* are eliminated but the pressure solutions become poor as β increases. The displacement solution loses its accuracy as β increases.

Acknowledgment

The support of Yonsei University is gratefully acknowledged.

References

- Babuška, I. (1971), "Error bounds for finite element method", *Numer. Math.*, **16**, 322-333.
- Brezzi, F. (1974), "On the existence, uniqueness and approximation of saddle-point problems arising from Lagrange multipliers", *RAIRO Ser. Rouge Anal. Numér.*, R-2, 129-151.
- Hughes, T.J.R. (1977), "Equivalence of finite elements for nearly incompressible elasticity", *J. Appl. Mech.*, **44**, 181-183.
- Hughes, T. J. R. and Franca, L. P. (1987), "A new finite element formulation for computational fluid dynamics: VII. The Stokes problem with various well-posed boundary conditions: Symmetric formulations that converge for all velocity/pressure spaces", *Comput. Meths. Appl. Mech. Engrg.*, **65**, 85-96.
- Lee, R. L., Gresho, P. M. and Sani, R. L. (1979), "Smoothing techniques for certain primitive variable solutions of the Navier-Stokes equations", *Internat. J. Numer. Meths. Engrg.*, **14**, 1785-1804.
- MacNeal, R.H. (1993), *Finite Elements: Their Design and Performance*, Marcel Dekker Inc., New York.
- Malkus, D.S. and Hughes, T.J.R. (1978), "Mixed finite element methods-reduced and selective integration technique: a unification of concepts", *Comput. Meths. Appl. Mech. Engrg.*, **15**, 63-81.

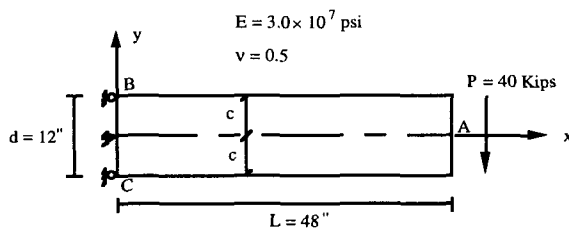


Fig. 1. Timoshenko beam bending problem

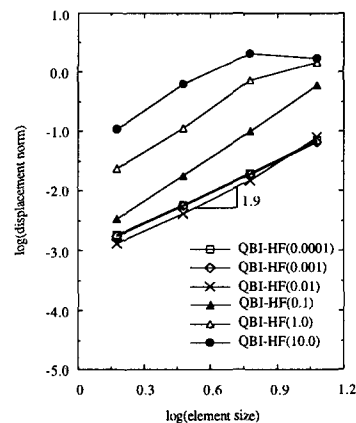


Fig. 2. Convergence rates of displacement norms in QBI-HF

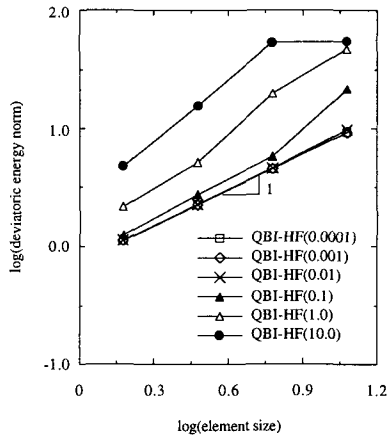


Fig. 3. Convergence rates of deviatoric energy norms in QBI-HF

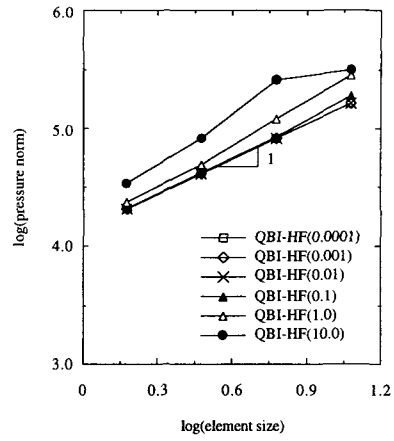


Fig. 4. Convergence rates of pressure norms in QBI-HF

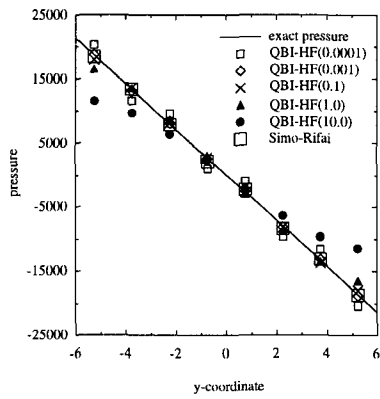


Fig. 5. Pressure distributions with the prescribed displacement boundary condition (QBI-HF)

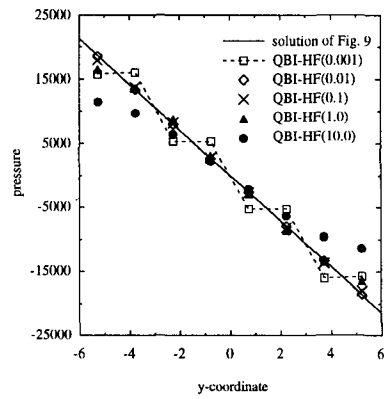


Fig. 6. Pressure distributions with the prescribed displacement boundary condition and the perturbed displacement boundary condition (QBI-HF)

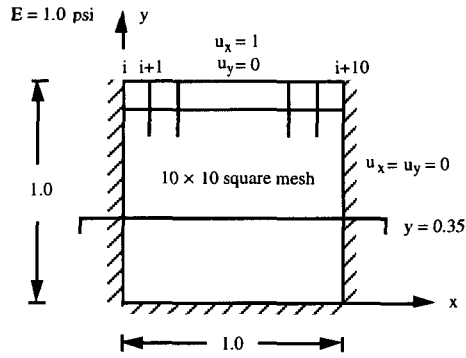


Fig. 7. Driven cavity flow model

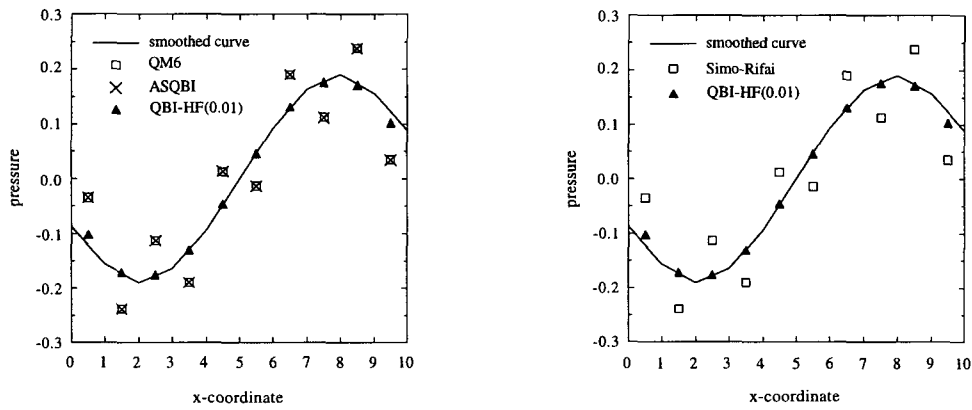


Fig. 8. Pressure distributions at $y = 0.35$ in the driven cavity flow problem with the boundary condition Case A ($\nu = 0.4999$ in QM6, Simo-Rifai, and ASQBI; $\nu = 0.5$ and $\beta = 0.01$ in QBI-HF)

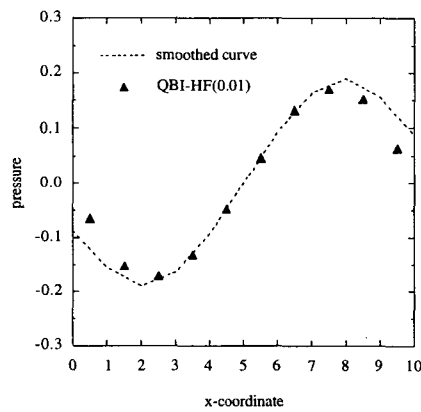


Fig. 9. Pressure distributions at $y = 0.35$ in the driven cavity flow problem with the boundary condition Case B ($\nu = 0.5$ and $\beta = 0.01$ in QBI-HF).
* Simo-Rifai and other elements show severe *pressure modes*.